

# Down regulation of talin alters cell adhesion and the processing of the $\alpha 5\beta 1$ integrin

Corinne Albigès-Rizo, Philippe Frachet and Marc R. Block\*

Laboratoire d'Etude des Systèmes Adhésifs Cellulaires, URA CNRS 1815, Université J. Fourier, B.P. 53X, F38041 Grenoble Cedex, France

\*Author for correspondence

## SUMMARY

The role of talin was addressed by down regulating its expression using an antisense RNA strategy. HeLa cells were transfected with a talin 5' cDNA fragment under the control of the inducible human metallothionein promoter. Isolated clones displayed a decrease in talin level down to 10% of control. The reduction in talin expression dramatically slowed down the kinetics of cell spreading. Mock-transfected cells, spread out onto fibronectin, exhibited large peripheral adhesion plaques. In contrast, cells with reduced talin expression showed smaller focal contacts localized all over the ventral face, and displayed a marked decrease in the number of stress fibers. Immunoprecipitation experiments carried out with a polyclonal antibody on surface-labeled receptor indicated a shift in the mobility for both  $\alpha 5$  and  $\beta 1$  subunits. Surprisingly,  $\beta 1$  integrin chains

could not be detected by indirect immunofluorescence using monoclonal antibodies in talin deficient clones. Western blot analysis indicated the presence of two forms of  $\beta 1$ . We analyzed the processing of  $\beta 1$  in normal and talin deficient cells using pulse chase experiments. Normal cells required a minimum of 5 hours for the processing of mature  $\beta 1$ , while the talin deficient AT22 clone showed that the  $\beta 1$  precursor was slowly converted into a very low molecular mass product. Our data demonstrate that talin plays a central role in the establishment of cell-matrix contacts. In addition, down regulation of talin impairs the folding and processing of  $\beta 1$  integrins.

Key words: antisense RNA, cell adhesion, focal adhesion, integrin, metallothionein promoter, talin,  $\beta 1$  integrin processing

## INTRODUCTION

Cell adhesion to extracellular matrix occurs through highly organized cellular structures named focal contacts, focal adhesions, or adhesion plaques (Woods and Couchman, 1988; Burridge et al., 1988; Beckerle and Yeh, 1990). Adhesion plaques are the transmembrane links formed via integrin receptors between the extracellular matrix and the cytoskeleton. The organization of this linkage has not yet been unravelled and is consequently poorly understood (Luna and Hitt, 1992). Some members of the integrin receptor family participate in the organization of focal contacts, whereas other members or other isoforms have never been found to be associated with these structures (Balzac et al., 1993). Furthermore heterogeneity in the composition of adhesion plaques has been suggested (Tranqui et al., 1993). On CHO cells grown onto fibronectin two types of contacts with distinct structural organizations and dynamics have been described: highly dynamic peripheral adhesion plaques which initiate stress fibers and more static thinner central contacts which are organized at an early stage in the adhesion process. The integrins are a large family of heterodimeric ( $\alpha\beta$ ) transmembrane receptors (for review see Sastry and Horwitz, 1993). The C-terminal cytoplasmic domain of the  $\beta$  chain interacts directly with specific cytosolic proteins such as talin and  $\alpha$ -actinin (Burridge et al.,

1988; Otey et al., 1990). Conversely, the cytoplasmic C-terminal domain of the  $\alpha$  subunit seems to control the ligand-dependent localization of integrin heterodimers into focal contacts (Briesewitz et al., 1993a). In addition to this structural role, recent data suggest that the clustering of integrins also plays an important role in outside-in signalling through the tyrosine kinase pp125 FAK (Schaller et al., 1992; Schaller and Parsons, 1993). Our increasing knowledge about the interactions of integrins with the extracellular matrix contrasts with the paucity of information on the proteins localized into focal contacts, their respective interactions, and their connections made with actin stress fibers. A number of proteins including talin, vinculin, tensin, paxillin, zyxin and  $\alpha$ -actinin, are known to contribute to the overall organization of focal contacts (Burridge et al., 1988). Recent findings suggest a possible implication of focal contacts in outside-in and/or inside-out signalling. For example, some proteins such as paxillin, tensin and pp125FAK become phosphorylated in response to cell adhesion to ligands of the extracellular matrix (Burridge et al., 1992; Bockholt and Burridge, 1993). The possible role of vinculin in the regulation of adhesion was recently addressed by the overexpression and suppression of vinculin in normal and transformed cells (Rodriguez Fernandez et al., 1992, 1993). Modulation of vinculin expression modifies the shape,

motility and adhesion-dependent growth ability of the cell, but has little effect on cell adhesion.

The ability of talin to interact with both cytoskeletal and membrane-associated proteins suggests that talin is involved in the establishment of transmembrane connections between the actin cytoskeleton and the extracellular environment. Such links occur at sites of cell-substratum adhesion. Thus, talin has potentially a key role in the formation of focal adhesions. Talin is a large protein with an apparent molecular mass of 235 kDa in mammals, composed of 2,541 amino acids, as deduced by Rees et al. (1990) from mouse cDNA sequence. Talin binds the cytoplasmic domain of the  $\beta 1$  and  $\beta 3$  integrin subunits and is associated with other cytoskeletal proteins such as vinculin (Horwitz et al., 1986; Sastry and Horwitz, 1993) and actin (Muguruma et al., 1990). Previous studies involving the microinjection of a monoclonal antibody into cells revealed that talin is required for the assembly of focal adhesions (Nuckolls et al., 1992). In addition to its obvious structural role, talin has a number of other intriguing features. It is a substrate of the  $\text{Ca}^{2+}$  activated protease calpain II found concentrated into focal contacts (Beckerle et al., 1987). Two proteolytic fragments of 47 kDa and 190-200 kDa are generated. Cleavage occurs at a specific site (Rees et al., 1990) for membrane associated talin whereas cytosolic talin remains intact (Tranqui and Block, 1995). The physiological significance of this cleavage remains unclear. Phosphorylation of the 47 kDa calpain N-terminal fragment of talin has been proposed as a possible signalling mechanism (Bertagnolli et al., 1993; Simons and Elias, 1993).

In order to study the effect of reduced talin expression on cell behavior, HeLa cells were transfected with an episomal inducible vector that controls the expression of a 5' fragment of talin cDNA in the antisense orientation. This fragment was obtained from a  $\lambda$ gt10 cDNA library screened with talin cDNA probe generated by RT/PCR on CHO cells. Two clones displaying a decrease in talin levels down to 10% of the controls were isolated. The phenotype of these clones suggested that talin is involved in the focal adhesion assembly and is required for the maturation and folding of the integrin with the  $\beta 1$  subunit.

## MATERIALS AND METHODS

### Materials

Monoclonal antibodies: anti-chicken talin (8d4), anti-human vinculin (hVIN1) and anti-actin against the C-terminal actin fragment were purchased from Sigma (St Louis, MO); the monoclonal anti-human  $\beta 1$  antibody K20 and the anti- $\alpha 5$  antibody (SAM-1) from Immunotech (Marseille, France). Polyclonal antibodies: anti-human  $\beta 1$  was obtained from Chemicon (Temecula, CA) and the anti- $\alpha 5\beta 1$  from Gibco BRL (Gaithersburg, MD). For western blotting, the anti-human vinculin (V284) used was from Boehringer (Mannheim, Germany). Oligonucleotides were synthesized by Appligene (Strasbourg, France) or Eurogentec (Seraing, Belgium). RNA was isolated according to the method of Gough (1988). DNA amplification was performed on a Dry Block PHC-3 (Techne, Inc). The partial talin cDNA was obtained from a CHO  $\lambda$ gt10 cDNA library (Clontech, Palo Alto, CA). The cDNA fragments obtained by polymerase chain reaction and the  $\lambda$ gt10 cDNA fragments were analyzed by double stranded plasmid DNA sequencing using the Sequenase kit (USB, Cleveland, OH).

### Cell culture and DNA transfection

HeLa cells were from the Pasteur Institute, France. Cells were cultured in  $\alpha$ -MEM supplemented with 10% heat inactivated fetal calf serum and 2 mM glutamine at 37°C in a 5%  $\text{CO}_2$  atmosphere.

For DNA transfection,  $0.5 \times 10^6$  cells were seeded in 100 mm tissue culture dishes, grown overnight, and transfected with a total of 10  $\mu\text{g}$  of plasmid using Transfectam (IBF, France). Adsorption and uptake of plasmid were carried out for 6 hours at 37°C. The day after transfection, the cells were split 1:10 or 1:50 and seeded. 24 hours later they were transferred into the selection medium containing 500  $\mu\text{g}/\text{ml}$  of hygromycin (Sigma, St Louis, MO). After 10-20 days individual clones were isolated and expanded.

### Plasmid construction

According to the sequence of mouse talin published by Rees et al. (1990) and based on the well-conserved amino acid sequences between mouse and hamster, two oligonucleotides were used as PCR primers to generate a fragment of talin cDNA surrounding an ATG region: primer Tal-1 5'CGTGAGCGGATCCCAGAGGCC3' and primer Tal-2 5'TTCCGTCTAACATCCGGATC3'. Briefly, reverse transcription was carried out on total CHO RNA in 20  $\mu\text{l}$  of buffer using 5 units of Moloney murine reverse transcriptase (Gibco BRL) and the primer Tal-2. The final volume during the amplification including the upstream primer Tal-1 was 100  $\mu\text{l}$  after addition of all components. PCR thermal cycles were performed as follows: denaturation was performed at 94°C for 2 minutes, annealing at 50°C for 2 minutes, and polymerization at 70°C for 2 minutes. The reaction was initiated by adding 2.5 units of Taq DNA polymerase (Boehringer Mannheim Biochemicals), after which 40 thermal cycles were carried out as described above. The PCR reaction products were separated by agarose gel electrophoresis and the 192 bp DNA fragment was extracted by electroelution. The resulting DNA was blunt-ended, subcloned into the *Sma*I site of pBluescript SK- (Stratagene, La Jolla, CA) for sequencing and used as a probe labeled with  $^{32}\text{P}$  for the ensuing screening of the CHO  $\lambda$ gt10 cDNA library. The positive clones were purified by the plate lysate method (Maniatis et al., 1982). A cDNA fragment was isolated by *Eco*RI digestion. The resulting 0.9 kb fragment included 0.3 kb of the 5' untranslated region and 0.6 kb of the coding region. A few differences between the nucleotide sequence of mouse and hamster talin were observed (manuscript in preparation). The cDNA fragment was purified by electroelution, blunt-ended and inserted either into the *Sma*I-digested and dephosphorylated pBluescript SK- vector or into the *Pvu*II-digested and dephosphorylated pMEP4 vector (Invitrogen Corp., Leek, Netherlands) in an antisense orientation. pMEP4 is an episomal vector conferring hygromycin resistance. Transcription of the cDNA is controlled by the inducible human metallothionein II gene enhancer/promotor while a termination signal is provided by the SV40 poly(A). The talin antisense expression vector was named pMEP4/AT2.

### Episomal DNA preparation and Southern blotting

Episomal DNA was prepared by cell lysis with 0.6% SDS, 10 mM EDTA for 20 minutes. Then, 1 M NaCl was added and the mixture incubated for 5 hours. Two extractions with phenol/chloroform and ethanol precipitations were subsequently performed (Seed and Aruffo, 1987). One tenth of the preparation was used for PCR amplification with 2 oligonucleotide primers Tal-1 (bases matching the insert sequence) and oligonucleotide 667 5'CCGCGTGCAACCTGTCC3' (bases matching the vector sequence). PCR amplification was carried out for 30 thermal cycles as previously described. PCR products were separated by electrophoresis on a 1.2% agarose gel.

### Talin antisense RNA detection

Cytoplasmic RNA was digested with Promega RNase free DNase according to the manufacturer's procedure in order to eliminate contaminating DNA. Messenger RNA (corresponding to 2  $\mu\text{g}$  of total

RNA) was reverse transcribed to prepare first strand cDNA. The reaction was performed for 45 minutes at 37°C with 100 units of reverse transcriptase (BRL) using the following primer, 5'AAGCT-GCCACCATGGTTGCGC3', which is complementary to the antisense RNA. In a control experiment the enzyme was omitted. Then in order to amplify the fragment extending from nt -11 to nt 318 the PCR was performed with the previous primer and another corresponding to the complementary strand: 5'TCTTGAGTCATC-CACCATG3'. Amplification steps were carried out using the following program repeated 22 times: 1 minute at 94°C, 1 minute at 50°C, 1.5 minutes at 72°C, then one final extension step at 72°C for 4 minutes. Amplification products were submitted to electrophoresis on a 1.5% agarose gel and transferred to a Nylon Hybond N+ membrane (Amersham) according to the manufacturer's recommendations. Detection of amplified fragments was carried out with <sup>32</sup>P-random priming labelled cDNA probes using the rapid hybridization buffer (Amersham) according to the supplier's instructions. The talin DNA probe used to detect the amplified product corresponded to the PCR fragment generated from the plasmid pMEP4AT2 with Tal1 and Tal2 (5'AAGCTGCCATGGTTGCGC3' and 5'TCTTGAGTCATC-CACCATG3'). After extensive washes, the membrane was autoradiographed.

### Pulse-chase experiments

Protein processing and turnover rates on adherent HeLa cells were determined by pulse chase labeling. Cells were seeded onto 35 mm plates, then incubated for 1 hour at 37°C in methionine and cysteine free DME medium (Sigma). At the end of this incubation the medium was replaced with fresh labeling medium containing 200 µCi/ml [<sup>35</sup>S]methionine and [<sup>35</sup>S]cysteine (Pro-mix<sup>TM</sup> L-<sup>35</sup>S in vitro cell labeling mix, Amersham). After 60 minutes at 37°C the labeling medium was withdrawn, the cells were washed three times with normal growth medium and cultured for varying times in the same medium. The cells were washed twice with phosphate buffered saline (PBS), and directly lysed on plates at the indicated time points. Immunoprecipitation was performed with the polyclonal anti-β1 antibody directed against the cytosolic domain of the β1 subunit as described below. Precipitated immune complexes were resuspended in 50 µl of nonreducing Laemmli buffer and the proteins were separated by electrophoresis on a 7.5% SDS polyacrylamide gel. The gels were fixed for 30 minutes in 10% acetic acid and 25% isopropanol, then treated with a fluorographic reagent (EN3HANCE; NEN Research products). The gels were dried under vacuum at 80°C for 1 hour and exposed to autoradiograph film (Hyperfilm-MP, Amersham).

### Lysis and immunoprecipitation

HeLa cells from a 100 mm tissue culture dish were harvested with trypsin/EDTA. Then, the cells were washed twice with PBS and lysed for 1 hour at 4°C in RIPA buffer (1% NP40, 0.5% deoxycholic acid, 0.1% SDS, 150 mM NaCl, 50 mM Tris-HCl, pH 8) containing 1 mM MgCl<sub>2</sub>, 1 mM CaCl<sub>2</sub>, 10 µM pepstatin A, 10 µg/ml leupeptin and 1 mM PMSF. After clarification of the cell lysates by centrifugation at 11,000 g for ten minutes at 4°C, the protein concentration was determined. Immunoprecipitation was performed by incubation with the selected antibody for 2 hours at 4°C. The antigen antibody complexes were bound to Protein G during an incubation period of 1 hour at 4°C with 20 µl of 50% (v/v) Protein G agarose beads (Calbiochem) in suspension in the lysis buffer. Before use, the beads were blocked with a protein extract from HeLa cells. The beads were washed three times with RIPA buffer before loading onto a gel.

### PAGE and immunoblotting

Cell lysates or immune complexes were separated by SDS-PAGE under non reducing conditions. Proteins were transferred to nitrocellulose by electroblotting using a semi-dry apparatus (Bio-Rad). Talin, β1 subunit of integrin, actin or vinculin were detected on the blots

with the appropriate monoclonal antibodies, followed by anti-mouse IgG or anti-rabbit IgG coupled to horseradish peroxidase. Detection was achieved using a chemiluminescent probe (ECL; Amersham). Several exposures of the blots to X-ray films were quantitated using a video enhanced analyzer and the 1.55 NIH Image public domain software.

### Cell surface biotinylation

Cells were surface-labeled with biotin using a modification of a previously described method (Isberg and Leong, 1990). Adherent cells were harvested with trypsin/EDTA, washed twice with PBS and adjusted to 5×10<sup>6</sup>/ml in 0.9% NaCl and 20 mM Hepes, pH 7.8, containing 1.5 mg/ml of biotin (NHS-LC-Biotin, Pierce). Following a 30 minute incubation at 4°C with constant agitation, cells were washed three times in PBS and pellets of cells subjected to lysis and immunoprecipitation as described above. Immunoprecipitated proteins were resuspended in 30 µl of nonreducing sample buffer and separated by a 7.5% SDS-polyacrylamide gel electrophoresis. Transfer was performed as described above. Following transfer, the membrane was blocked in TBS/5% dried skimmed milk powder. The membrane was incubated with horseradish peroxidase-conjugated streptavidin (Boehringer Mannheim, diluted 1:5,000 in TBS/0.05% Tween-20/5% dried skimmed milk powder) for 1 hour and washed four times in TBS/0.05% Tween-20. Biotinylated proteins were visualized by chemiluminescence (ECL, Amersham).

### Endoglycosidase F digestion

After cell-surface labeling with biotin, HeLa cells were lysed in RIPA buffer, and α5 and β1 polypeptides were immunoprecipitated. The immune complexes were washed three times in lysis buffer, rinsed once in endoglycosidase F buffer (50 mM KPO<sub>4</sub>, pH 7, 50 mM EDTA, 0.2% SDS, 0.5% Triton X-100) and resuspended in 60 µl of endoglycosidase F buffer. Then, the samples were split into two 30 ml aliquots. To one aliquot, 5 ml (2 units) of endo F (Boehringer Mannheim) were added. To the other aliquot, 5 µl of buffer alone was added for mock digestion. The complexes were incubated at 37°C for 22 hours. After digestion, SDS-PAGE sample buffer was added and the complexes were heated at 100°C for 5 minutes.

### Indirect immunofluorescence

Cells were grown overnight on coverslips pre-coated with fibronectin, then rinsed three times with PBS, and fixed with 3% paraformaldehyde in PBS containing 2% sucrose, for 10 minutes, at 37°C. When required, the cells were permeabilized at room temperature using 300 mM sucrose, 50 mM NaCl, 3 mM MgCl<sub>2</sub>, 1% NP-40, 20 mM Hepes, pH 7.4, for 30 minutes (Dejana et al., 1988). After one wash with PBS, cells were incubated with primary antibodies in PBS containing 1% BSA and 0.05% Tween-20 for 1 hour at 37°C. The cells were then washed four times with PBS/Tween-20 and incubated for another hour with rhodamine or FITC-conjugated goat anti-rabbit or anti-mouse antisera in PBS containing 1% BSA and 0.05% Tween-20 at 37°C. The coverslips were washed with PBS/Tween-20 and mounted onto glass slides in a Mowiol mounting solution. The slides were examined with a Nikon Microphot FxA microscope equipped for epifluorescence.

### FACS analysis

Cells were harvested with 1 mM EDTA, 0.1% Trypsin (w/v) and washed twice with PBS. The cells were fixed by 10 minutes incubation with 3% freshly prepared paraformaldehyde in PBS. The immune reaction was performed for 30 minutes at 4°C with the appropriate primary monoclonal antibody in Hanks' balanced salt solution (HBSS) containing 0.3% saponin. It was followed by an incubation with the anti-IgG fluorescein-conjugated antibody (Jackson) in Hanks' buffer containing 0.1% saponin. At each stage, the cells were washed three times in HBSS containing 0.1% saponin. Immunofluorescence staining was analyzed on a FACScan flow cytometer

(Becton Dickinson) using a FACStar research software program (Lysis II). Background fluorescence was determined with a nonimmune mouse IgG control or a nonimmune rabbit antiserum. The data were displayed as cell number (ordinate) versus log fluorescence (abscissa). Quantification of fluorescence was done from acquisition in the linear mode and mean fluorescence intensity was expressed in FACS arbitrary values.

### Adhesion assays

To determine cell adhesion on different substrates, nontreated 35 mm plates were coated with 10 µg/ml of vitronectin, laminin, or fibronectin for 2 hours at 37°C as previously described (Tranqui et al., 1992). Coating with collagen was done for 2 hours at 4°C to avoid its denaturation. Cell attachment ( $5 \times 10^4$  cells per plate) took place at 37°C for 6 hours or 16 hours. Adherent cells were photographed under phase contrast and counted as flattened or round. The number of cells in a constant unit area (0.003 mm<sup>2</sup>) was estimated. All adhesion assays were run in triplicate. For each sample 2 areas were counted. Laminin, vitronectin and collagen are purchased from Sigma. Fibronectin was purified from bovine plasma according to the method of Engvall and Ruoslahti (1977).

## RESULTS

### Production of HeLa cell lines transfected with talin antisense cDNA

HeLa cells were transfected with the episomal vector pMEP4/AT2 designed to produce antisense talin RNA under control of the inducible human metallothionein II promoter (see Materials and Methods). The 0.9 kb λgt10 talin cDNA fragment inserted into the pMEP4 vector included 0.3 kb of

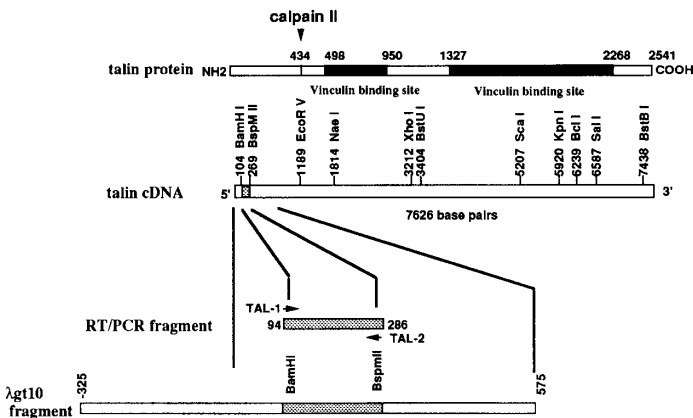


**Fig. 1.** Cloning strategy. The primary structure of talin deduced from the complete sequence of the mouse protein (Rees et al., 1990) is shown and the site of cleavage by calpain II into two proteolytic fragments (between residues 433-434) is indicated. Black boxes represent the two putative vinculin binding sites (Gilmore et al., 1992). The positions of some of the unique restriction sites are indicated with vertical lines above the cDNA of talin. According to the published sequence, two oligonucleotides (TAL-1 and TAL-2) were designated to generate the probe by RT/PCR (dotted box) which was used for the screening of ATG-containing talin cDNA fragments. The talin fragment isolated from the λgt10 library contains 0.3 kb of the 5' untranslated sequence followed by 0.6 kb of the 5' translated sequence. The whole of this fragment was cloned into the expression vector pMEP4 in the antisense orientation.

the 5' untranslated region, the ATG start codon and the 0.6 kb of the translated sequence (Fig. 1). After 10 days of transfection, 50 hygromycin-resistant colonies were selected. Numerous HeLa clones appeared to be hygromycin-resistant at first glance but turned out to die after the second screening: they did not resist long-term culture with antibiotic. Among the resistant clones, two of them (designated HeLa/AT21 and HeLa/AT22, respectively), contained the episomal pMEP4/AT2 plasmid and were further characterized. Identification of the vector was performed using the polymerase chain reaction (PCR). The results are shown in Fig. 2. Briefly, amplification was carried out using the vector extracted from the transfected HeLa cells as a matrix, and the primers 667 and

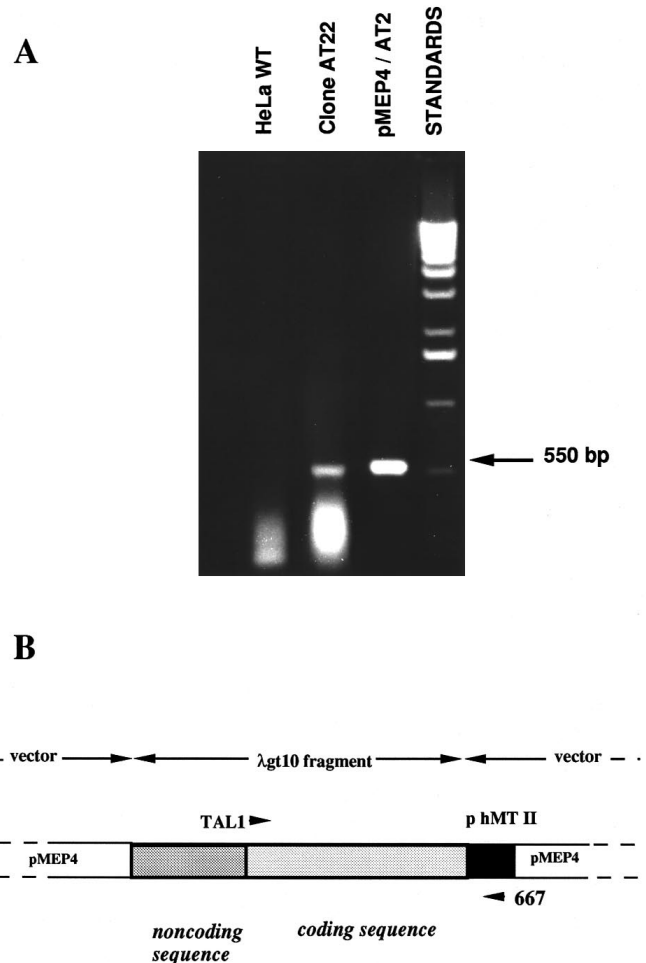


**Fig. 2.** PCR screening of the transfected clones. (A) PCR reactions were performed on a DNA preparation designed to extract any episomal vector from HeLa cells. From the left, lane 1 is a negative control using nontransfected HeLa cells. In lane 2 HeLa cells transfected with pMEP4/AT2 are used (clone HeLa/AT22). A PCR product in the QUIAGEN-purified expression vector pMEP4/AT2 constitutes the positive control (lane 3). It generates the expected fragment of 550 bp. 20 µl aliquots of 50 µl reactions are run on a 1.2% agarose gel. Lane 4 contains the molecular size markers (1 kb ladder, BRL). (B) The oligonucleotides TAL-1 and 667 are localized on talin cDNA and parental pMEP4 expression vector, respectively. The black box represents the human metallothionein II promoter which controls the transcription of talin fragment in the antisense orientation (gray box).

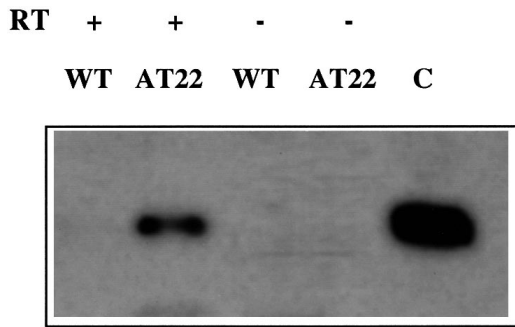


**Fig. 3.** Talin antisense RNA detection. Total RNA was purified from wild-type HeLa cells or AT22 cells. After RT/PCR amplification, a 329 bp DNA fragment generated from the talin antisense mRNA was detected by Southern blot hybridization using a [ $^{32}$ P]talinal DNA probe only in the case of AT22 cells. The RT/PCR DNA fragment was not detected when the reaction was performed without reverse transcriptase. Positive control (C) corresponds to the PCR amplification of pMEP4/AT2 plasmid.

Tal-1 matching the MTH promoter sequence and the insert sequence, respectively (Fig. 2B). Therefore, amplification of DNA could not occur from the endogenous talin gene which reveals that the  $\lambda$ gt10 talin cDNA fragment was truly inserted into the antisense position. This PCR generated the expected fragment of 550 bp (Fig. 2A) identical to the PCR-fragment produced from a control reaction using the original expression vector pMEP4/AT2. Conversely, under the same experimental conditions, we were unable to generate this fragment either with wild-type HeLa cells or with pMEP4-transfected HeLa cells.

Expression of the talin antisense RNA was determined by a RT/PCR reaction (Fig. 3) using an oligonucleotide complementary to the expected antisense RNA for the first strand synthesis. The generated 329 bp fragment was detected after hybridization with a talin specific probe (189 bp) synthesized by PCR. This 329 bp fragment is localized between nt -11 and nt 318 whereas the probe is from nt 96 to nt 285 (relative to the translation initiation). This 329 bp fragment was present in the AT22 clone but not in wild-type HeLa cells or when hybridized to products generated by PCR without reverse transcriptase. GAPDH mRNA amplification was used as an internal control in each reaction (data not shown).

#### Down regulation of talin expression in transfected cells

Western blot experiments and flow cytometry analysis of HeLa/AT22 or AT21 cells disclosed an important decrease in talin expression compared to wild-type HeLa cells or pMEP4-transfected HeLa cells (mock transfected). Flow cytometry analysis was carried out with fixed and saponin-permeabilized cells after an incubation with the monoclonal anti-talin primary antibody 8d4 followed by a secondary fluorescent anti-mouse (Fab')<sub>2</sub>. An important decrease in the fluorescence of HeLa/AT22 cells as compared to pMEP4 transfected cells was observed (Fig. 4A). Overnight addition of cadmium chloride to the culture medium resulted in a further decrease in the fluorescence of HeLa/AT22 cells (Fig. 4B) but there was no effect on pMEP4 transfected HeLa cells, i.e. mock-transfected cells (not shown). Quantification of the FACS results for

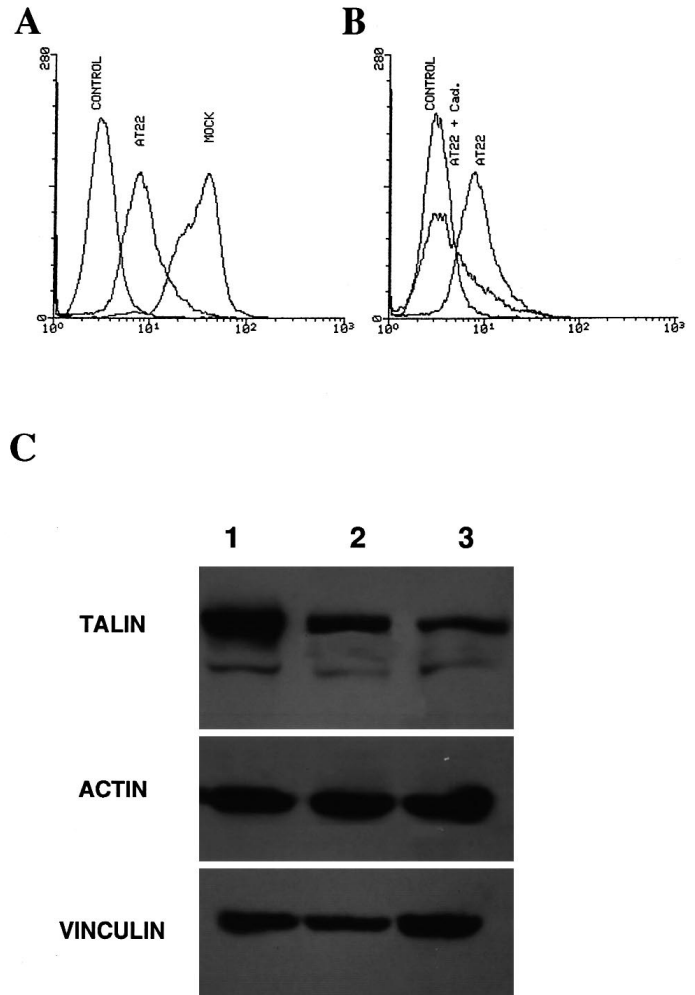


**Fig. 4.** Down regulation of talin expression in antisense talin-transfected cells. (A and B) Flow cytometry analysis of mock-transfected and HeLa/AT22 cells. (A) A decrease in talin expression is observed in AT22 cells as compared to mock transfected cells. (B) The same experiment performed with 10  $\mu$ M of cadmium added. (C) Talin, actin, vinculin expression with (3) or without (2) cadmium induction (12 hours at 10  $\mu$ M) into HeLa/AT22 cells are compared with the synthesis of these same proteins in mock transfected cells (1). Equal amounts of total cell protein lysates (50  $\mu$ g) are separated by SDS-PAGE and blotted onto nitrocellulose. The staining of talin, actin and vinculin was performed with appropriate antibodies followed by ECL detection of the anti-mouse-HRP IgG secondary antibody.

HeLa/AT22 indicated a decrease, compared to mock transfected cells, of 90% and 80% in the talin related fluorescence with or without cadmium induction, respectively (Table 1). On western blot experiments performed with 50  $\mu$ g of proteins from whole-cell extracts (Fig. 4C and Table 1) and 8d4 anti-talin antibody, AT22 cells displayed a decrease in talin synthesis whereas levels of other cytoskeletal proteins such as vinculin and actin were not altered. After the normalization of the data using actin expression, the densitometry of the stained band corresponding to talin indicated a decrease in talin content of about 60% and 38% compared to talin levels in mock transfected cells, with or without cadmium induction, respectively (Table 1). Similar figures were obtained with

**Table 1. Expression of talin in normal and mutant HeLa cells**

Cell type	FACS	Western blot	Metabolic labeling
	Fluorescence intensity %	Densitometry %	Radioactivity %
HeLa mock	100	100	100
HeLa mock + Cd <sup>2+</sup>	90±5	n.d.	n.d.
HeLa/AT22	20±2	62	46
HeLa/AT22 + Cd <sup>2+</sup>	8±2	40	20

HeLa/AT21 cells (not shown). After metabolic labeling and talin immunoprecipitation, quantification given by a phosphorimager showed a decrease in talin content of 80% and 54% compared to talin levels in mock transfected cells, with or without cadmium, respectively (Fig. 5 and Table 1). Indeed, these data indicated that our antisense talin construct efficiently and specifically down regulated talin expression in HeLa cells. Although basal level transcription of the human metallothionein II promoter was relatively high and gave an already significant decrease in talin expression without any induction, the addition of cadmium to the culture medium further decreased the intracellular talin level.

### Phenotype and adhesive properties of HeLa/AT clones

As the presence of our antisense DNA construct did perturb the expression of talin in HeLa cells, we evaluated their degree of spreading on different substrates. Untreated 35 mm dishes were coated with collagen, laminin, vitronectin and fibronectin at a concentration of 10 µg/ml in PBS as described in Materials and Methods. Although the morphologies of anti-talin expressing cells and wild-type cells varied widely, the cells were simply sorted into two categories: either round or spread-out. The number of cells of each type was counted at 1 hour, 6 hours and 16 hours after the beginning of adhesion at 37°C. A cell was scored as spread-out if it displayed a thin lamella while cells lacking these structures were scored as round. Usually the latter group of cells were surrounded by a phase-light region or refringent region. Spread cells could be maintained for 3 days at 37°C without subsequent morphological modifications.

Cell spreading kinetics differ depending on the substrate and were fastest on fibronectin-coated dishes. After 6 hours, 65% of spread cells were counted on fibronectin whereas on laminin, vitronectin and collagen they reached only 40%, 10%, and 15%, respectively (Fig. 6A,B). Under identical experimental conditions, wild-type or mock transfected HeLa cells achieved almost complete spreading on fibronectin within 15 minutes. Phase contrast microscopy at high magnification revealed that the cells of antisense transfected clones (with a reduced talin level) were poorly spread onto the substrates. Conversely, mock-transfected cells expressing normal talin levels spread normally and had a typical morphology indistinguishable from that of the wild-type cells. After 48 hours at 37°C, full spreading of HeLa/AT cells was almost achieved on all the substrates tested but collagen. With this latter substrate, 85% of the cells kept a round morphology (Fig. 6A). However, a targeted reduction in talin expression was sufficient for conferring changes in cell shape even on fibronectin. The trans-

fecting cells were attached but poorly spread on the substrate (Fig. 6A). Addition of cadmium at non lethal concentration induced the rounding up of HeLa/AT cells seeded onto tissue culture treated plastic within 16 hours, but has no effect on wild-type HeLa or mock transfected HeLa under our experimental conditions (Fig. 7).

### Analysis of focal adhesions and cytoskeletal organization in HeLa/AT cells

It is noteworthy that most cells displaying a round morphology were lost from the coverslip during the process of fixation, permeabilization and immunostaining. Consequently, immunofluorescence microscopy revealed only cells displaying a spread-out morphology. Furthermore, when round cells were still present on the coverslip at the end of the immunostaining process, we were unable to detect any organization of focal adhesions. Thus the immunostaining experiments were performed with cells spread on fibronectin for 48 hours without cadmium. Under these experimental conditions, we knew that the basal level of the metallothionein promoter was high enough to induce both a reduction in spreading capacity and down regulation of talin expression. In mock-transfected HeLa cells, talin and vinculin were found in focal adhesion localized mainly at the cell margins (Fig. 8A,C). Identical patterns were observed with wild-type cells (not shown). On the other hand, immunostaining of talin and vinculin revealed that the organization of focal adhesions was strongly modified in HeLa/AT cells (Fig. 8B,D). Double staining of AT22 cells showed a colocalization of talin and vinculin (Fig. 9) indicating that these small adhesion plaques still constituted both proteins. While mock-transfected HeLa cells had large peripheral adhesion plaques incorporating β1 integrin chains (Fig. 8E), the HeLa/AT cells exhibited a large number of smaller focal adhesions localized all over the ventral face. Surprisingly, the HeLa/AT clones gave no immunostaining with the K20 anti-β1 monoclonal antibody (Fig. 8F). The staining of actin microfilaments by fluorescein-conjugated phalloïdin showed a cortical actin network and a much reduced number of stress

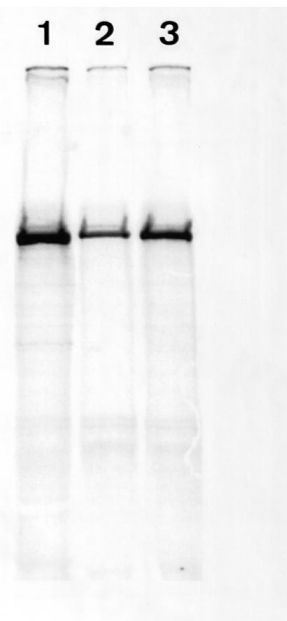


**Fig. 5.** Immunoprecipitation of talin after metabolic labeling. Following metabolic labeling with [<sup>35</sup>S]methionine and [<sup>35</sup>S]cysteine (50 µCi/ml) for 3 hours, the cells were lysed with RIPA buffer. Talin was subsequently immunoprecipitated with the monoclonal antibody 8d4 from equal amounts of proteins of total cell lysates determined by micro BCA assay. Lane 1, talin from control cells; lane 2, talin from induced AT22 cells; lane 3, talin from non induced AT22 cells.

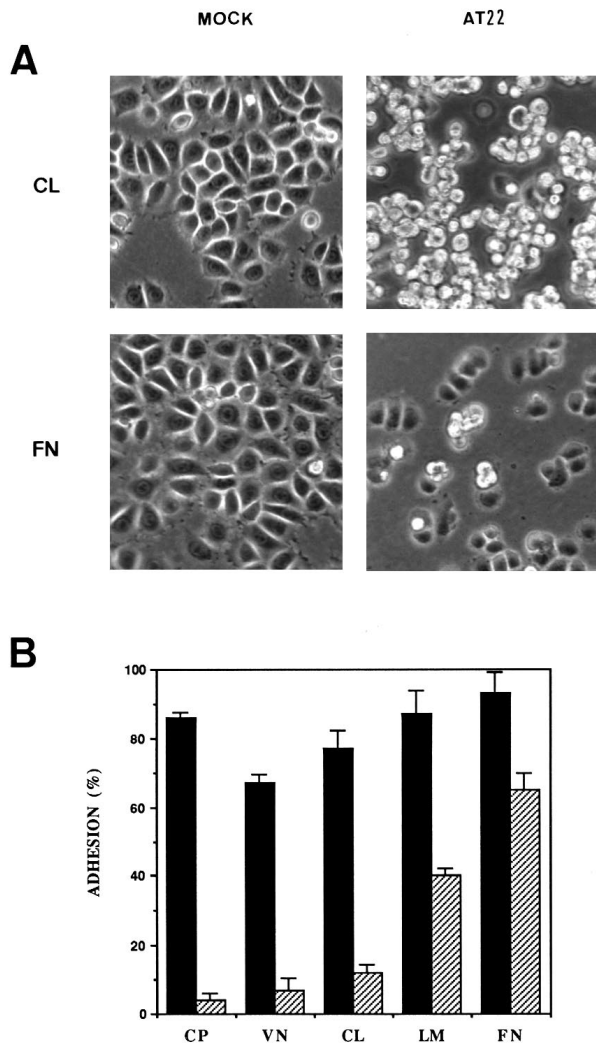


**Fig. 6.** Inhibition of cell spreading in HeLa cells transfected by the antisense construct pMEP4/AT2. (A) Phase contrast micrographs showing spreading of mock-transfected or HeLa/AT22 cells on collagen (CL) or fibronectin (FN) after 16 hours of adhesion at 37°C. (B) Cells are allowed to attach and spread for 16 hours at 37°C onto tissue culture treated plastic (CP), collagen (CL), laminin (LM), vitronectin (VN) and fibronectin (FN). The amount of spread-out cells is determined as described in Materials and Methods. Mock-transfected cells (black columns) are compared to HeLa AT 22 cells (hatched columns).

fibers at the periphery of the talin deficient cells (Fig. 8H) compared to control cells (Fig. 8G).

### The $\beta 1$ integrin subunit is present at the surface of talin deficient cells in a distinct conformational state

The lack of  $\beta 1$  detection observed by immunostaining (Fig. 8F) was confirmed by FACS analysis using the same monoclonal antibody (K20) directed against the extracellular domain of the  $\beta 1$  subunit (Fig. 10). Another anti- $\beta 1$  monoclonal antibody (clone P4C10-Gibco-BRL) was assayed and gave an identical result (data not shown). Immunoprecipitation experiments were carried out with a polyclonal antibody on surface labeled receptor using both wild-type and AT22

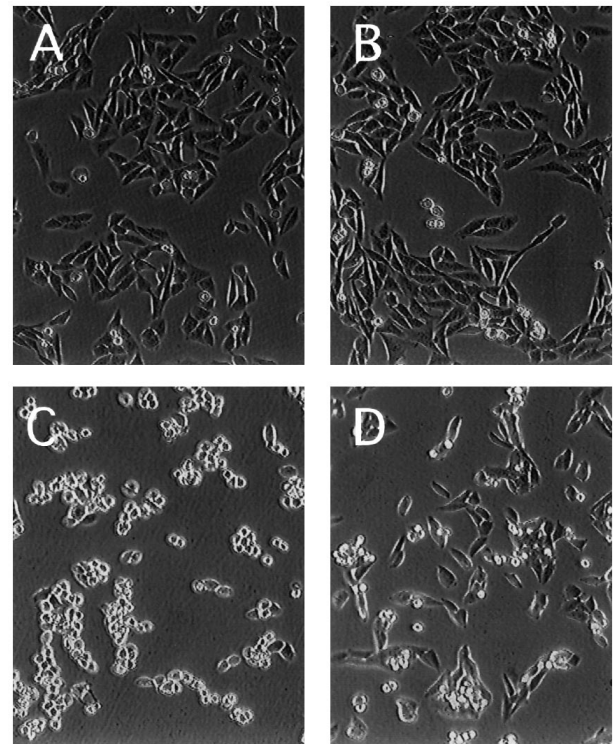


**Fig. 7.** Cell rounding and detachment of AT22 cells caused by induction with cadmium. Mock HeLa cells (A,B) and AT22 cells (C,D) were cultured in the absence (B,D) or in the presence (A,C) of cadmium (5  $\mu$ M) and examined under a phase contrast microscope. Addition of cadmium induced a rounding up of the AT22 cells at 16 hours followed by the complete detachment of cells from the substratum at 20 hours (C) whereas no effect on the shape of the control cells was detected (A).

cells. On wild-type HeLa cells,  $\alpha 5$  and  $\alpha 1$  subunits coimmunoprecipitated with the  $\beta 1$  chain. Conversely, in the AT22 clone, both  $\alpha 5$  and  $\beta 1$  subunits underwent processing events that resulted in shifts to lower relative molecular mass (Fig. 11). These abnormal chains were named  $\alpha'5$  and  $\beta'1$ , respectively. There was no major change in the total amounts of fibronectin receptor subunits expressed and inserted into the plasma membrane. Altogether these data indicated that  $\beta'1$  in association with  $\alpha'5$  was still present at the surface of talin deficient cells. However, the  $\beta'1$  as well as  $\alpha'5$  subunit appeared to be modified since there was loss of epitopes recognized by several monoclonal antibodies and a mobility shift on SDS-PAGE. We tried to detect the presence of the  $\alpha'5$  subunit at the cell surface of the HeLa/AT22 cells spread-out onto fibronectin (Fig. 12). A monoclonal antibody raised against  $\alpha 5$  (clone SAM1) revealed that this subunit was localized into focal adhesions (Fig. 12A). The same levels of  $\alpha 5$  subunit were found by FACS analysis on HeLa/AT, or mock transfected cells (Fig. 12B,C).

Although Fig. 11 shows that the  $\alpha 1$  expression level was dramatically reduced, immunoprecipitation of surface labeled proteins with anti- $\alpha 1$  antibodies shows the still remaining  $\alpha 1$  subunit associated with the  $\beta 1$  chain. But in the same way  $\alpha 1\beta 1$  integrin shows a shift in the mobility on SDS-PAGE (not shown).

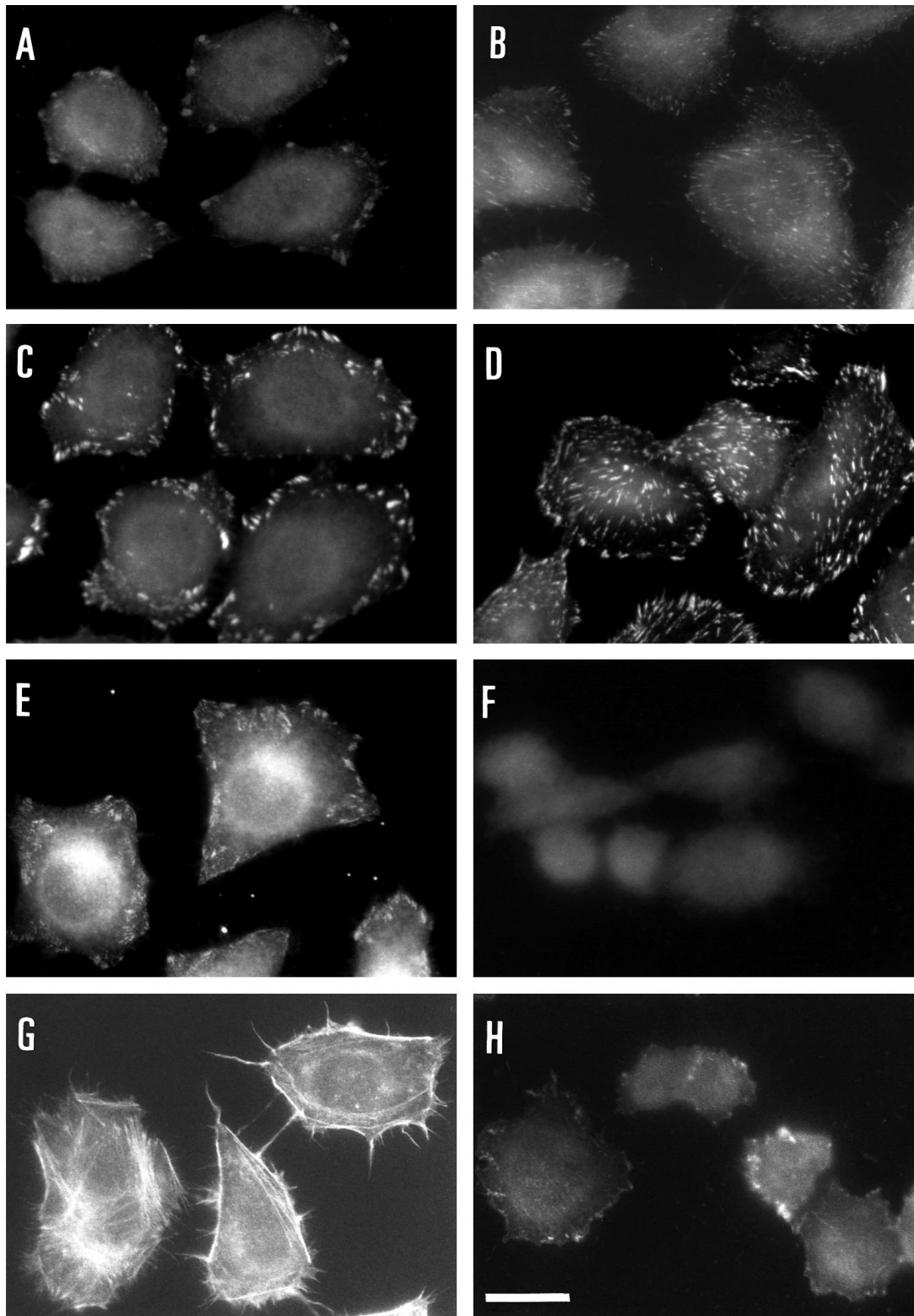


**Fig. 8.** Organization of the cellular structures in talin-deficient cells. Immunofluorescence distribution of talin (A,B), vinculin (C,D),  $\beta 1$  integrin (E,F) and actin (G,H), respectively, in mock-transfected HeLa cells (A,C,E,G) and HeLa/AT22 cells (B,D,F,H). Cells are allowed to attach onto a fibronectin-treated coverslip for 48 hours at 37°C. Then, they are fixed and permeabilized and allowed to react with primary antibodies for 1 hour at 37°C and subsequently with rhodamine-conjugated anti-mouse antisera for another hour. Talin (A) and vinculin (C) are concentrated at the cell margin in mock-transfected HeLa, whereas transfected cells show a great number of central plaques (B,D). The integrin chain  $\beta 1$  localized into focal adhesions by the monoclonal antibodies (K20) in mock-transfected cells (E) is no longer detected in the HeLa/AT22 cells (F). FITC-labeled phalloidin staining (G,H) reveals a reduced number of stress fibers. Bar, 20  $\mu\text{m}$ .

### Talin down regulation alters the processing of $\beta 1$ integrins

Western blot experiments were performed on cell lysates from mock, HeLa/AT21 or HeLa/AT22 cells, using a specific (affinity purified) polyclonal antibody raised against the cytosolic domain of  $\beta 1$  (Chemicon). Fig. 13 shows that, despite

the lack of its immunofluorescence detection, the  $\beta 1$  chain was still expressed by all these cells as described by immunoprecipitation experiments. Under non reducing conditions a single band corresponding to the apparent molecular mass of 130 kDa of  $\beta 1$  was detected in mock cell lysates with or without cadmium added. Conversely, without any cadmium added, two



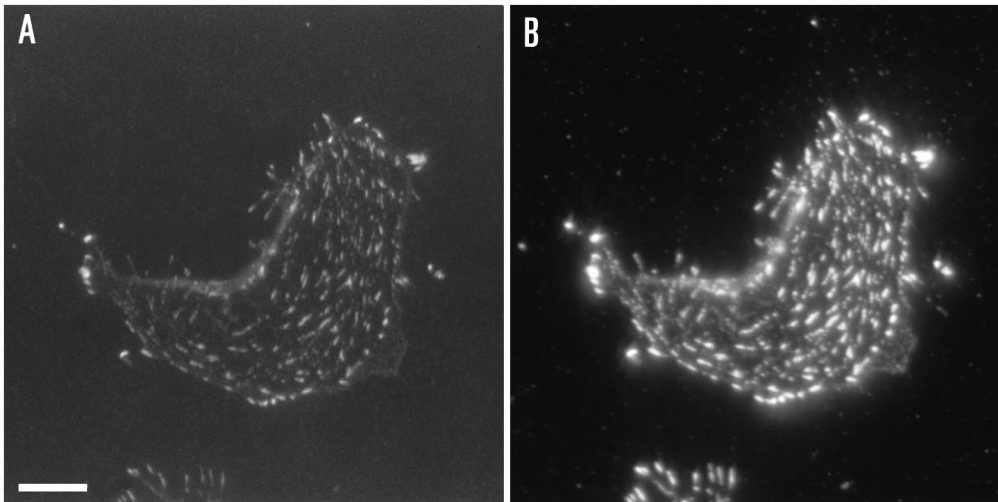


**Fig. 9.** Immunofluorescence microscopy showing double staining of talin and vinculin. AT22 cells were double labeled for talin (A) and for vinculin (B). Both proteins were colocalized all over the ventral face of the cell. Bar, 10  $\mu$ m.

bands were detected by the anti- $\beta$ 1 antibodies in both talin deficient HeLa/AT21 and AT22 clones (Fig. 13). The lower molecular mass chains might correspond to some forms of pro- $\beta$ 1 chains (Heino et al., 1989). Addition of cadmium for 24 hours to HeLa/AT cells resulted in a dramatic increase in the lower band and the complete loss of the higher chain (Fig. 13). A cell lysate of mock-transfected cells from a 24 hour culture in suspension was also analyzed (Fig. 13). A single 130 kDa chain was detected in this lysate. This indicated that the putative pro- $\beta$ 1 accumulation was not due to a defect in cell adherence. In all the cells tested with or without cadmium induction, no significant changes in  $\beta$ 1 RNA levels were found as compared to GAPDH mRNA levels taken as internal controls (not shown). Thus, a decrease in talin expression did not affect expression of the  $\beta$ 1 gene. The hypothesis that the  $\beta$ 1 integrin was not processed correctly in talin deficient cells was investigated with non-induced cells by pulse-chase experiments (Fig. 14). The pulse-chase experiments followed by the immunoprecipitation of the  $\beta$ 1 chain with an anti-C-terminal domain (Chemicon) indicated that normal cells required a minimum of 5 hours to allow the conversion of pro- $\beta$ 1 (100 kDa) into mature  $\beta$ 1 (130 kDa). Conversely, AT22 cells showed a progression of a  $\beta$ '1 precursor form with an apparent molecular mass of approximately 100-110 kDa into a new form of  $\beta$ '1 with very low molecular mass of about 90 kDa. Presumably, this end product corresponded to the accumulated  $\beta$ 1 form detected by western blot analysis upon cadmium addition. As indicated in pulse chase experiments, AT22 cells showed

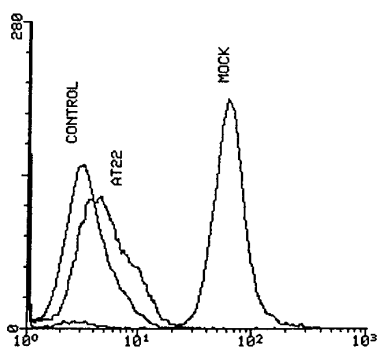


**Fig. 10.** FACS analysis of the  $\beta$ 1 integrin subunit in HeLa/AT cells. The expression in permeabilized mock-transfected and HeLa/AT22 cells is assayed by flow cytometry. The cells are stained with the anti- $\beta$ 1 monoclonal antibody K20. A negative control performed with a non specific mouse IgG is shown.

the conversion of pro $\beta$ '1 into  $\beta$ '1 but never the maturation of the pro $\beta$ '1 into  $\beta$ 1. Consequently, the protein doublet detected in AT cells by western blot (without cadmium induction) might correspond to the pro $\beta$ '1 and the  $\beta$ '1.

Pulse chase experiments also indicated that in wild-type HeLa cells pro $\alpha$ 5 and pro $\alpha$ 1 coimmunoprecipitated with pro $\beta$ 1 and were converted into  $\alpha$ 5 and  $\alpha$ 1 subunits, respectively, in about 3 hours. For AT22 cells, a lower molecular mass  $\alpha$  band coimmunoprecipitated with pro $\beta$ '1 and was identified as a modified pro  $\alpha$ '5 subunit (Fig. 14). This chain was quickly processed (1 hour) into abnormal lower molecular mass  $\alpha$ '5.

#### Decrease in talin results in partial glycosylation of fibronectin receptor

To determine whether the modification of integrin processing was related to a defect in glycosylation, immunoprecipitates of cell-surface-biotinylated  $\alpha$ 5 and  $\beta$ 1 were treated with endoglycosidase F and analyzed by SDS-PAGE under non reducing conditions. Endoglycosidase F, which cleaves both the high-mannose and complex forms of the N-linked oligosaccharides from the polypeptide backbone, induced a shift in the mobility of cell surface  $\alpha$ 5 and  $\beta$ 1. In wild-type

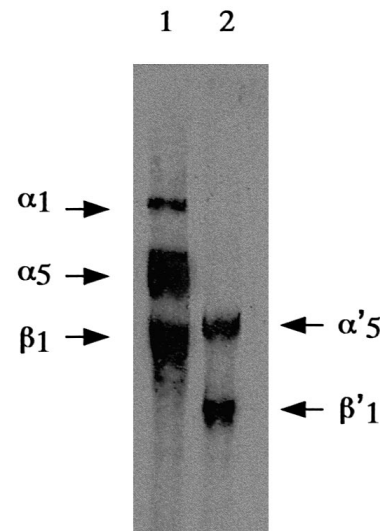


**Fig. 11.** Immunoprecipitation of surface biotinylated  $\alpha$ 5 $\beta$ 1 complexes. Proteins from mock-transfected cells (lane 1) and HeLa/AT22 cells (lane 2) are immunoprecipitated with an anti- $\alpha$ 5 $\beta$ 1 polyclonal antibody as described in Materials and Methods. The biotinylated protein bands are detected by streptavidin-HRP and the ECL chemiluminescence kit.

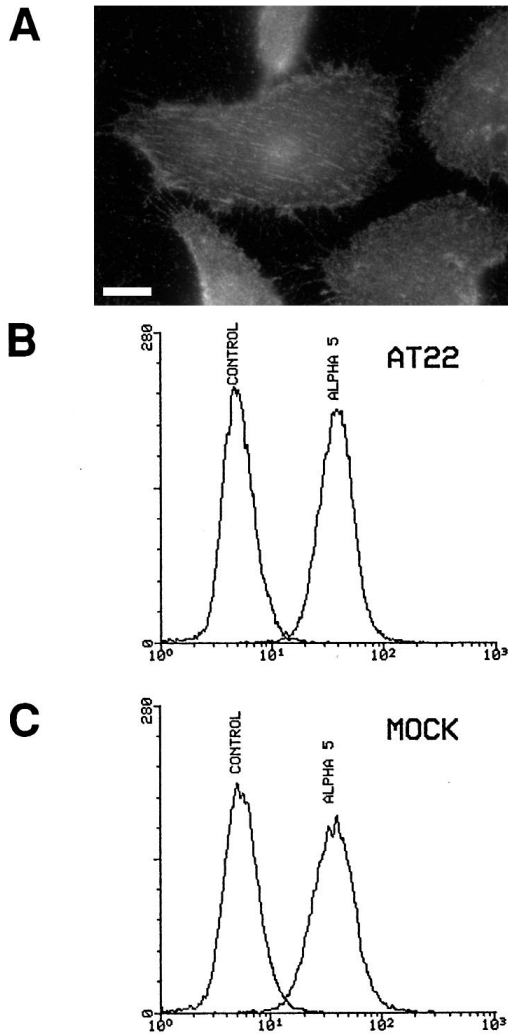


**Fig. 12.** Expression of  $\alpha 5$  integrin subunit on HeLa/AT22 cells. (A)  $\alpha 5$  integrin subunit is detected by immunofluorescence on adherent and permeabilized HeLa/AT22 cells. Bar, 10  $\mu\text{m}$ . Surface expression of  $\alpha 5$  is analyzed by FACS on HeLa/AT22 (B) or mock-transfected cells (C). The anti- $\alpha 5$  monoclonal antibody Sam-1 is used in all the experiments. Negative controls are shown.

HeLa cells, the apparent molecular masses of  $\alpha 5$  and  $\beta 1$  subunits drop from 155 kDa to 120 kDa and from 130 kDa to 90 kDa, respectively (Fig. 15, lanes 1, 2 and 3, 4), whereas in AT22 cells, the apparent molecular mass of  $\alpha 5$  was reduced from 135 kDa to 120 kDa (Fig. 15, lanes 5, 6) and for  $\beta 1$ , from 100 kDa to 90 and 80 kDa. Thus, treatment with endoglycosidase F yielded the same end product of 120 kDa for  $\alpha 5$  indicating that the defect in the processing of this subunit observed in AT2 clones was an incomplete N-glycosylation. On the other hand, endo F digestion of  $\beta 1$  produced a 90 kDa band found in both wild-type HeLa cells and AT22 clone and a 80 kDa band found solely in AT22. It is likely that the 90 kDa represents the unglycosylated  $\beta 1$ . Consequently, the 80 kDa band that accumulated in AT22 cells is a truncated  $\beta 1$ . For this latter subunit, the defect in the processing results from both partial glycosylation and proteolytic cleavage.

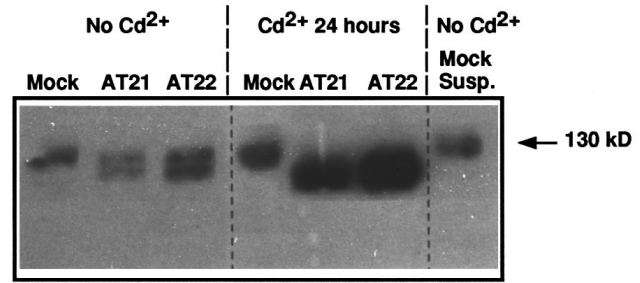


**Fig. 13.** Immunoblotting of the  $\beta 1$  subunit expressed into HeLa/AT cells. Equal amounts of total cell protein lysates (50  $\mu\text{g}$ ) from HeLa AT cells and mock transfected cells are separated by electrophoresis and blotted onto nitrocellulose. Lysates are provided from adherent cells or cells in suspension, with or without cadmium as indicated. Expression of  $\beta 1$  subunit is determined by incubation with the anti-human  $\beta 1$  polyclonal antibody followed by enhanced chemiluminescence detection with the goat anti-rabbit IgG horseradish peroxidase conjugate.

## DISCUSSION

An experimental approach using transfected HeLa cells with a 0.9 kb antisense talin cDNA (including a part of the 5' untranslated sequence) was designed to analyze the function of talin in cell adhesion and regulation. Since inhibition of expression of the proteins involved in cell adherence might be lethal, we chose the expression vector pMEP4. Upon cadmium addition, the human metallothionein II promoter drives the transcription of the antisense RNA from the inserted antisense talin cDNA. The origin of pMEP4 replication allowed a great number of episomal copies of the plasmid in HeLa cells. Therefore, high levels of antisense RNA required for the inhibition of expression of the targeted protein were produced. Indeed, when the construct was used to transfect CHO cells in which only replication of genome-integrated plasmid occurred, a very transient modification of cell adhesion was observed (personal unpublished data). After the transfection of HeLa cells, two independent clones containing the episomal vector were isolated and fully characterized. The clones exhibited identical phenotypes and were named HeLa/AT21 and AT22. Western blots as well as cytofluorimetric analysis and immunoprecipitation after metabolic labeling indicated that the level of talin could be reduced down to 10-40% of that normally found in wild-type or mock-transfected cells. This decrease was cadmium dependent, which indicates that down regulation was due to antisense RNA synthesis under the control of the hMT II promoter.

Our present results suggest that talin deficiency causes a defect in cell adherence. These cells not only spread poorly onto various substrates, but also show a dramatic decrease in their speed of adhesion and spreading (Fig. 6). Indeed, it took at least 48 hours at 37°C for these cells to be fully spread onto fibronectin (the most efficient substrate promoting adhesion of HeLa/AT cells), while only 15 minutes were required for wild-type HeLa cells and mock-transfected cells under identical conditions. After 48 hours at 37°C, the typical pattern of focal adhesion was markedly different in HeLa/AT clones compared to mock-transfected or wild-type cells (Fig. 8). Whereas normal cells exhibited a small number of large peripheral focal adhesions, HeLa/AT cells exhibited a large number of smaller

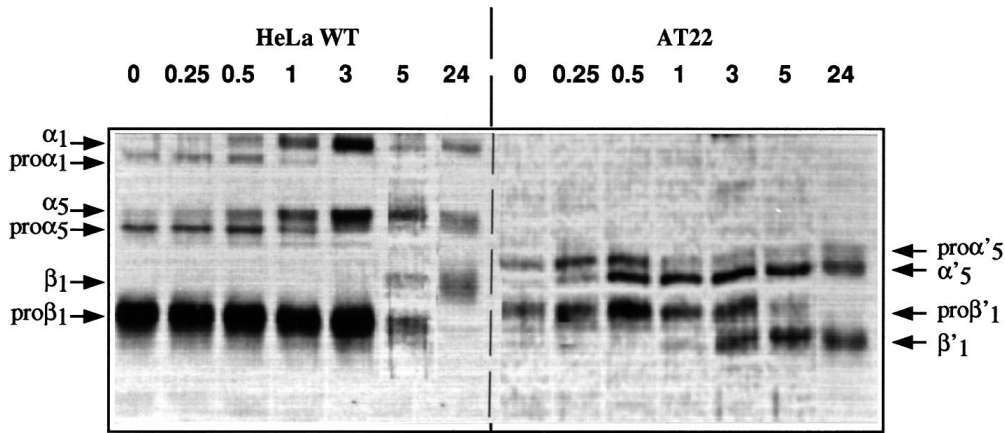


**Fig. 14.** Processing of  $\beta$ 1 integrins. Adherent cells were labeled for 1 hour with [ $^{35}$ S]cysteine and [ $^{35}$ S]methionine and chased in cold medium for the lengths of time indicated (chase times in hours). Cell extracts were immunoprecipitated with a polyclonal antibody to the  $\beta$ 1 integrin subunit. The left panel shows processing of  $\beta$ 1 integrins in wild-type HeLa cells whereas positions of abnormal  $\beta'$ 1 integrins are visualized on the right panel for talin deficient cells.

focal adhesions localized all over the ventral face. Adhesive structures in clones with decreased talin levels appeared to have an apparent normal structure as seen by immunofluorescence using antibodies against talin and vinculin. These patterns of large peripheral or small focal adhesions have been previously described as late and early stages of CHO cell adhesion, respectively (Tranqui et al., 1993). They were also observed in HeLa cells (not shown). Since the kinetics of adhesion were so slow with HeLa/AT cells, it is likely that the distribution of focal adhesions in these clones reflected solely an early stage of cell spreading rather than an abnormal organization. We suggest that, in talin deficient cells, the final state of spreading with large peripheral adhesion plaques could never be reached. With HeLa/AT cells, a straightforward interpretation of the slow kinetics of adhesion can be proposed: the recruitment of talin into focal adhesions may become a stringent limiting step because of the low amount of this protein in the cytosol. The role of talin in the establishment of focal adhesions suggested by our results is consistent with microinjection experiments using the anti-talin monoclonal antibody 8d4 (Nuckolls et al., 1992). Finally, a further decrease in talin expression by addition of cadmium induced the rounding up of AT21 and AT22 clones, whereas wild-type HeLa or mock transfected cells remained spread under identical experimental conditions. Similarly, down regulation of vinculin expression by antisense transfection confers a moderate defect in cell adhesion with smaller vinculin-positive plaques (Rodriguez-Fernandez et al., 1993). The organization of the cytoskeleton and focal contacts was also modified in HeLa/AT cells. Although these cells exhibited focal adhesions, fewer and shorter stress fibers remained, as though a high talin concentration were required for the nucleation of new stress fibers.

Surprisingly, the adhesion deficiency of HeLa/AT clones varied according to the extracellular matrix protein used (Fig. 6). These differences suggested that modifications of the integrin receptors might also occur upon down regulation of talin expression. Indeed, a loss of epitopes detected by immunofluorescence studies indicated that the  $\beta$ 1 chain was in a distinct conformational state named  $\beta'$ 1. The loss of detection was not due to a down regulation of  $\beta'$ 1 expression, since PCR did not reveal any significant changes in  $\beta'$ 1 mRNA levels and western blots showed that the chains were synthesized within the cells (Fig. 13). However, distinct  $\beta'$ 1 forms were found in

AT clones with lower apparent molecular masses that might correspond to precursors of  $\beta$ 1 (Heino et al., 1989; Hotchin and Watt, 1992). Abnormal processing of  $\beta'$ 1 integrins was confirmed by pulse chase experiments (Fig. 14). In wild-type HeLa cells normal processing of  $\beta$ 1 took at least 5 hours. Conversely, in the AT22 clone, at time zero the precursor of  $\beta'$ 1 was detected with a slightly higher molecular mass. This form was slowly converted into a low molecular mass form of the  $\beta$ 1 chain. The defect in  $\beta'$ 1 processing is probably a consequence of the genetic down regulation of talin since it was observed with the two independent clones HeLa/AT21 and HeLa/AT22 but not with mock-transfected HeLa cells. In the latter cells normal  $\beta$ 1 chains and no pro- $\beta$ 1 were immunodetected in western blots. Furthermore, when the expression of antisense RNA was induced by a non lethal concentration of cadmium, the abnormal lower molecular mass  $\beta'$ 1 form accumulated into HeLa/AT. Our results suggest that a more

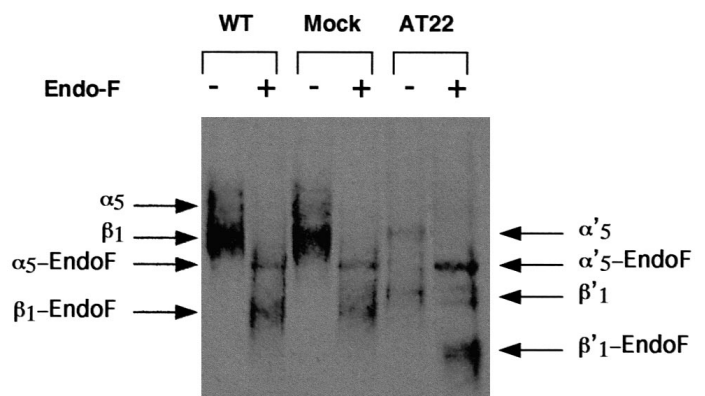


**Fig. 15.** Endoglycosidase F sensitivity of cell surface  $\alpha$ 5 $\beta$ 1 integrins. HeLa cells were surface-labeled with biotin, harvested with trypsin EDTA and subjected to lysis with RIPA buffer. Extracts were immunoprecipitated with anti- $\alpha$ 5 $\beta$ 1 polyclonal antibody (Gibco BRL) and incubated in the absence (-) or presence (+) of endo F as described in Materials and Methods. The immunoprecipitates were separated by SDS-PAGE under non reducing conditions and visualized using HRP streptavidin and the ECL chemiluminescence detection kit. Positions of  $\alpha$ 5,  $\beta$ 1 subunits and their respective endo F-digested forms are indicated at the left side for wild-type and mock HeLa cells. Integrin subunits detected in AT 22 cells are designated as  $\alpha'$ 5 and  $\beta'$ 1.

dramatic decrease in talin level resulted in the amplification of  $\beta'1$  processing defects. An alternative explanation for the modifications of the  $\beta'1$  chain could be the lack of adhesion with sufficient mechanical strength. Indeed, substrate adherence has been reported to modulate integrin gene expression and antigenic sites of the receptors (Frelinger et al., 1988; Chen et al., 1992). However, the observation that after 24 hours of culture in suspension, mock-transfected cells presented  $\beta 1$  chains indistinguishable from those of adherent mock-transfected cells, ruled out this hypothesis.

Pulse chase experiments indicated that  $\alpha 1$ ,  $\alpha 5$  and  $\beta 1$  subunits underwent processing events that resulted in shifts to a higher relative molecular mass, this suggesting that post-translational modifications were occurring. According to the treatment with endo-F, these modifications were mostly due to glycosylation. The same treatment performed on AT22 cells showed that the mobility shift for  $\beta'1$  and  $\alpha'5$  subunits compared to wild-type HeLa cells was due to partial glycosylation and also to proteolytic cleavage concerning the  $\beta'1$  chain. Furthermore, the monoclonal antibody K20 has been reported to recognize an epitope localized in the region 426-587 of the  $\beta 1$  chain (Takada and Puzon, 1993). This epitope is no longer recognized in the case of  $\beta'1$  integrin synthesized in AT22 cells, which is possibly related to the loss of glycosylation as 3 sites of potential N-linked glycosylation are localized in this region (Argraives et al., 1987). This would mean that the epitope bound by monoclonal antibody K20 developed relatively late during biosynthesis and needs post translational modification such as N-linked glycosylation in order to be recognized. Although  $\alpha'5\beta'1$  (and even  $\alpha'1\beta'1$ ; data not shown) synthesized in AT clones was abnormally processed, the low molecular mass final product reached the cell surface since it was detected after immunoprecipitation of the surface labeled proteins by anti- $\alpha 5\beta 1$ . Intermediate forms of the fibronectin receptor subunits were found on the surface of AT22 cells, hence complete processing of receptors into mature forms was not necessary for insertion into the plasma membrane. However, it must be pointed out that glycosylation might influence the receptor affinity for ligand on VLA integrins. As reported here, the molecular changes in the  $\beta'1$  subunit in HeLa/AT clones had only a limited influence on the final state of cell spreading onto laminin and fibronectin. Conversely, under identical experimental conditions, HeLa/AT spreading never occurred onto collagen which can be explained by the down regulation of the  $\alpha 1$  subunit (Fig. 11 and Fig. 14). The  $\beta 1$  integrin subunit is associated with various  $\alpha$  chains to form receptors for fibronectin ( $\alpha 4\beta 1$  and  $\alpha 5\beta 1$ ), laminin ( $\alpha 1\beta 1$ ,  $\alpha 2\beta 1$ ,  $\alpha 3\beta 1$  and  $\alpha 6\beta 1$ ), collagen ( $\alpha 1\beta 1$ ,  $\alpha 2\beta 1$ ,  $\alpha 3\beta 1$ , and  $\alpha 4\beta 1$ ) and vitronectin ( $\alpha v\beta 1$ ) (Hemler, 1990; Hynes, 1992). The coexistence of multiple  $\alpha$  subunits capable of assembly with a common  $\beta 1$  subunit to form a repertoire of integrin complexes with distinct adhesive specificities, and the fashion in which these complexes are assembled might be controlled by the glycosylation.

According to our data, down-regulation of talin seems to correlate with a defect in  $\beta 1$  integrin processing. This raises the possibility that talin could act as a chaperonin, helping the folding of integrin receptors that will be normally associated with it. This is apparently not consistent with the fact that some integrin heterodimers with deletions in the transmembrane and cytoplasmic domains have been successfully expressed into

host cells secreted in a functional soluble form (Briesewitz et al., 1993b). However, the total amount of the truncated integrin remains still very low compared to the level of expression of the normal protein (Frachet et al., 1992). Finally, biosynthetic studies using stable-expressing cell lines demonstrate that the soluble and the native heterodimers are formed independently. These studies strongly suggest that the cytoplasmic domains of  $\alpha$  and/or  $\beta$  subunits are involved in the assembly of native heterodimers (Briesewitz et al., 1993b). Our results add another piece of evidence in support of a role for talin in integrin assembly.

We thank Xavier Ronot for technical assistance in FACS analysis and helpful discussions. This work is supported in part by grants from the CNRS (ATiPE N° 900041) and from the Association pour la Recherche contre le Cancer.

## REFERENCES

- Argraives, W. C., Susuki, S., Arai, H., Thompson, K., Pierschbacher, M. D. and Ruoslahti, E. (1987). Amino acid sequence of the human fibronectin receptor. *J. Cell Biol.* **105**, 1183-1190.
- Balzac, F., Belkin, A. M., Kotliansky, V. E., Balabanov, Y. V., Altruda, F., Silengo, L. and Tarone, G. (1993). Expression of functional analysis of a cytoplasmic domain variant of the  $\beta 1$  integrin subunit. *J. Cell Biol.* **21**, 171-178.
- Beckerle, M. C., Burridge, K., DeMartino, G. N. and Croall, D. E. (1987). Colocalization of calcium-dependent protease II and one of its substrates at sites of cell adhesion. *Cell* **51**, 569-577.
- Beckerle, M. C. and Yeh, R. K. (1990). Talin role at sites of cell-substratum adhesion. *Cell Motil. Cytoskel.* **16**, 7-13.
- Bertagnolli, M. E., Locke S. J., Hensler, M. E., Bray, P. F. and Beckerle, M. C. (1993). Talin distribution and phosphorylation in thrombin-activated platelets. *J. Cell Sci.* **106**, 1189-1199.
- Bockholt, S. M. and Burridge, K. (1993). Cell spreading on extracellular matrix proteins induces tyrosine phosphorylation of tensin. *J. Biol. Chem.* **268**, 14565-14567.
- Briesewitz, R., Kern, A. and Marcantonio, E. (1993a). Ligand-dependent and -independent integrin focal contact localization: the role of the  $\alpha$  chain cytoplasmic domain. *Mol. Biol. Cell* **4**, 593-604.
- Briesewitz, R., Epstein, M. R. and Marcantonio, E. (1993b). Expression of native and truncated forms of the human interin  $\alpha 1$  sbunit. *J. Biol. Chem.* **268**, 2989-2996.
- Burridge, K., Fath, K., Kelly, T., Nuckolls, G. and Turner, C. (1988). Focal adhesion: Transmembrane junctions between the extracellular matrix and the cytoskeleton. *Annu. Rev. Cell Biol.* **4**, 487-525.
- Burridge, M. D., Turner, C. E. and Romer, L. H. (1992). Tyrosine phosphorylation of paxillin and pp125fak accompanies cell adhesion to extracellular matrix - a role in cytoskeletal assembly. *J. Cell Biol.* **119**, 893-903
- Chen, D., Magnuson, V., Hill, S., Arnaud, C., Steffensen, B. and Klebe, R. J. (1992). Regulation of integrin gene expression by substrate adherence. *J. Biol. Chem.* **267**, 23502-23506.
- Dejana, E., Colella, S., Conforti, G., Abbadini, M., Gaboli, M. and Marchisio, P.-C. (1988). Fibronectin and vitronectin regulate the organization of their respective Arg-Gly-Asp adhesion receptors in cultured human endothelial cells. *J. Cell Biol.* **107**, 1215-1223.
- Engvall, E. and Ruoslahti, E. (1977). Binding of soluble form of fibroblast surface protein, fibronectin, to collagen. *Int. J. Cancer* **20**, 1-5.
- Frachet, P., Duperray, A., Delachanal, E. and Marguerie, G. (1992). Role of the transmembrane and cytoplasmic domains in the assembly and surface exposure of the platelet integrin GPIIb/IIIa. *Biochemistry* **31**, 2408-2415.
- Frelinger, III, A. L., Lam, S. C.-T., Plow, E. F., Smith, M. A., Loftus, J. C. and Ginsberg, M. H. (1988). Occupancy of an adhesive glycoprotein receptor modulates expression of an antigenic site involved in cell adhesion. *J. Biol. Chem.* **263**, 12397-12402.
- Gilmore, A. P., Jackson, P., Waites, G. T. and Critchley, D. R. (1992). Further characterisation of the talin binding site in the cytoskeletal protein vinculin. *J. Cell Sci.* **103**, 719-731.

- Gough, N. M.** (1988). Rapid and quantitative preparation of cytoplasmic RNA from small numbers of cells. *Anal. Biochem.* **173**, 93-95.
- Heino, J., Ignatz, R. A., Hemler, M. E., Crouse, C. and Massagué J.** (1989). Regulation of cell adhesion receptors by transforming growth factor- $\beta$ . *J. Biol. Chem.* **264**, 380-388.
- Hemler, M. E.** (1990). VLA proteins in the integrin family: structures, functions, and their role on leucocytes. *Annu. Rev. Immunol.* **8**, 365-400.
- Horwitz, A., Duggan, E., Buck, C., Beckerle, M. C. and Burridge, K.** (1986). Interaction of plasma membrane fibronectin receptor with talin - a transmembrane linkage. *Nature* **320**, 531-533.
- Hotchin, N. A. and Watt, F. M.** (1992). Transcriptional and post-transcriptional regulation of  $\beta$ 1 integrin expression during keratinocyte terminal differentiation. *J. Biol. Chem.* **267**, 14852-14858.
- Hynes, R. O.** (1992). Integrins: Versatility, modulation and signalling in cell adhesion. *Cell* **69**, 11-25.
- Isberg, R. R. and Leong, J. M.** (1990). Multiple  $\beta$ 1 chain integrins are receptors for invasins, a protein that promotes bacterial penetration into mammalian cells. *Cell* **60**, 861-871.
- Luna, E. J. and Hitt, A. L.** (1992). Cytoskeleton-plasma membrane interactions. *Science* **258**, 955-963.
- Maniatis, T., Fritsch, E. and Sambrook, J.** (1982). *Molecular Cloning: A Laboratory Manual*. Cold Spring Harbor Laboratory Press, Cold Spring Harbor, NY.
- Muguruma, M., Matsumura, S. and Fukazawa, T.** (1990). Direct interaction between talin and actin. *Biochem. Biophys. Res. Commun.* **171**, 1217-1223.
- Nuckolls, G. H., Romer, L. H. and Burridge K.** (1992). Microinjection of antibodies against talin inhibits the spreading and migration of fibroblasts. *J. Cell Sci.* **102**, 723-752.
- Otey, C. A., Pavalko, F. M. and Burridge K.** (1990). An interaction between  $\alpha$ -actinin and the  $\beta$ 1 integrin subunit in vitro. *J. Cell Biol.* **111**, 721-729.
- Rees, D. J. G., Ades, S. E., Singer, S. J. and Hynes, R. O.** (1990). Sequence and domain structure of talin. *Nature* **347**, 685-689.
- Rodriguez Fernandez, J. L., Geiger, B., Salomon, D., Sabanay, I., Zoller, M. and Ben-Ze'ev, A.** (1992). Suppression of tumorigenicity in transformed cells after transfection with vinculin cDNA. *J. Cell Biol.* **119**, 427-438.
- Rodriguez Fernandez, J. L., Geiger, B., Salomon, D. and Ben-Ze'ev, A.** (1993). Suppression of vinculin expression by antisense transfection confers changes in cell morphology, and anchorage dependent growth of 3T3 cells. *J. Cell Biol.* **122**, 1285-1294.
- Sastry, S. K. and Horwitz, A. F.** (1993). Integrin cytoplasmic domains: mediators of cytoskeletal linkages and extra- and intracellular initiated transmembrane signalling. *Curr. Opin. Cell Biol.* **5**, 819-831.
- Schaller, M. D., Borgman, C. A., Cobb, B. S., Vines, R. R., Reynolds, A. B. and Parsons, J. T.** (1992). Pp 125 fak, a structurally distinctive protein-tyrosine kinase associated with focal adhesion. *Proc. Nat. Acad. Sci. USA* **89**, 5192-5196.
- Schaller, M. D. and Parsons, J. T.** (1993). Focal adhesion kinase: an integrin-linked protein tyrosine kinase. *Trends Cell Biol.* **3**, 258-262.
- Seed, B. and Aruffo, A.** (1987). Molecular cloning of the CD2 antigen, the T-cell erythrocyte receptor, by a rapid immunoselection procedure. *Proc. Nat. Acad. Sci. USA* **84**, 3365-3369.
- Simons, P. C. and Elias, L.** (1993). The 47kD fragment of talin is a substrate for protein kinase P. *Blood* **82**, 3343-3349.
- Takada, Y. and Puzon, W.** (1993). Identification of a regulatory region of integrin  $\beta$ 1 subunit using activating and inhibiting antibodies. *J. Biol. Chem.* **268**, 17597-17601.
- Tranqui, L., Soyoz, S. and Block, M. R.** (1992). An in vitro model giving access to adhesion plaques. *In Vitro Cell. Dev. Biol.* **28A**, 17-23.
- Tranqui, L., Usson, Y., Marie, C. and Block, M. R.** (1993). Adhesion of CHO cells to fibronectin is mediated by functionally and structurally distinct adhesion plaques. *J. Cell Sci.* **106**, 377-387.
- Tranqui, L. and Block, M. R.** (1995). Talin processing occurs within adhesion plaques. *Exp. Cell Res.* **217**, 149-156.
- Woods, A. and Couchman, J. R.** (1988). Focal adhesions and cell-matrix interactions. *Relat. Res.* **8**, 115-182.

(Received 20 January 1995 - Accepted 30 June 1995)